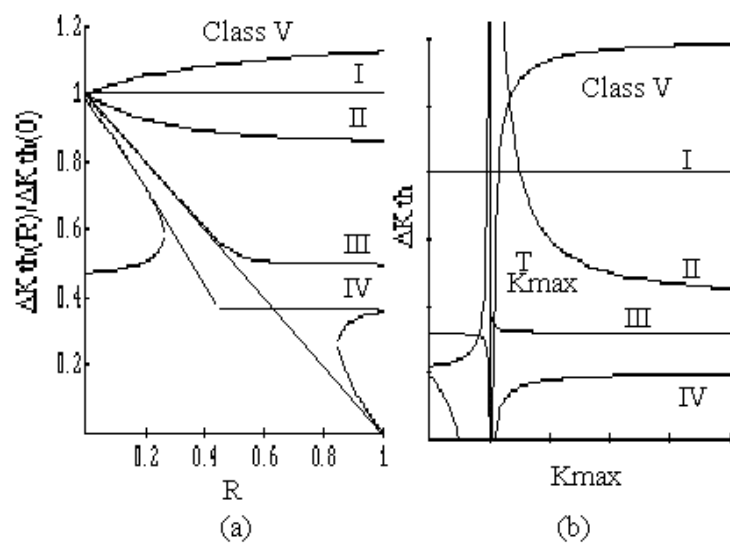


## Cyclic and Static Fatigue Crack Growth Thresholds

G.S.Wang



SWEDISH DEFENCE RESEARCH AGENCY

Aeronautical Division  
SE-172 90 Stockholm

FOI-R-- 0787--SE

January 2003

ISSN 1650-1942

**Scientific Report**

# **Cyclic and Static Fatigue Crack Growth Thresholds**

**Geng-Seng Wang**

# Cyclic and Static Fatigue Crack Growth Thresholds

G.S.Wang

Aeronautics Division, The Swedish Defence Research Agency, SE-172 90 Stockholm, Sweden,  
telephone: +46-8-555 04 488, telefax: +46-8-25 89 19, email: [wgs@foi.se](mailto:wgs@foi.se)

## **Abstract**

Mathematical foundation for the new double threshold concept is investigated for the analysis of fatigue crack growth. The model consists of two major elements; an intrinsic crack growth threshold which corresponds the material resistance to the fatigue crack growth due to the reverse yielding at the crack tip, and a maximum stress intensity factor threshold which contributes to the possible change of crack growth mode and the crack closure mechanism when the tensile plastic deformation ahead of crack tip is very small. These two thresholds are proposed as material parameters to determine fatigue threshold condition. The mathematical model is developed based on the double threshold concept so that only three parameters are required to determine the threshold for various different materials. The model is successfully used to characterise the crack growth threshold for varieties of materials with significantly different features. The model is also randomised to account for the scatter in fatigue crack growth thresholds. The statistical model has successfully accounted for and explained the widely observed phenomenon that the scatter in the experimentally measured thresholds may increase considerably for low stress ratios.

Key words: Fatigue Crack Growth, Thresholds, R ratios, Statistics, Stress Effect

## **Contents**

Introduction .....	1
Features of the threshold .....	3
Mathematical formulations.....	5
Applications.....	8
Statistical feature .....	12
Concluding remarks.....	17
Acknowledgement.....	18
References .....	19

## **Introduction**

Since Paris and Erdogan proposed the range of stress intensity factor for the cyclic load as a governing parameter for the analysis of fatigue crack growth rate, the relation has been extensively used in the analysis of fatigue crack growth problems even if the load is of the random nature. The use of Paris/Erdogan law has the advantage that a similarity may be achieved so that material data obtained in the laboratory using small specimens may be used to analyse the fatigue crack growth in structures so long as the fracture mechanics parameter, the stress intensity factor, can be solved both for the specimens and for the structures containing cracks.

A schematic of Paris/Erdogan type of crack growth rate against stress intensity factor range for the constant amplitude loading at different stress ratios is shown in Fig.1. To various different extents, the crack growth rate has usually been observed to be higher for high stress ratio (R ratio) than for low stress ratio for the same stress intensity factor range for various materials. Empirical fittings has been tried to account for the stress ratio effect. Such fittings are, however, unsuccessful when being used for variable amplitude loading because load interaction has a strong effect on the fatigue crack growth behaviour.

The discovery of the crack closure phenomenon<sup>1 2</sup> has successfully solved many problems concerning the fatigue crack growth behaviour such as the stress ratio effect, load interaction effect, and even part of the small crack effect. The crack closure is mainly determined by the mechanically irreversible plastic deformation, the metallurgical irregularities (roughness), and the environment chemical reaction (oxidation and corrosion etc.). For the intermediate range (Region II, the so-called the Paris region shown in Fig.1) where the stress intensity factor can be used as a crack growth driving force, the plastic deformation induced crack closure is a major contribution affecting the cyclic plastic deformation at the crack tip in many applications. Further increase of stress intensity range into Region III shown in Fig.1 will lead to an interaction between the fatigue crack growth mechanism and the static crack failure mechanism. The fatigue life in the region usually occupies small part of the total fatigue life. For most applications, simplification can be accepted by using interpolation between Region II fatigue crack growth data and static crack failure data such as R-curve or simply the fracture toughness.

Region I shown in Fig.1 is an important part of the fatigue crack growth analysis since the fatigue life within this region may occupy a significant part of the total life. In addition, a threshold has been observed for many materials that the fatigue crack growth

rate may be significantly reduced from the slope in Region II. When the stress intensity factor range is close to the threshold, a rapid decrease of the crack growth rate may occur and the crack may stop growing. It is necessary to correctly define the threshold for a given material in the analysis of its fatigue crack growth for the constant amplitude loading with small stress ranges, or for the variable amplitude loading with large number of small cycles close to the threshold.

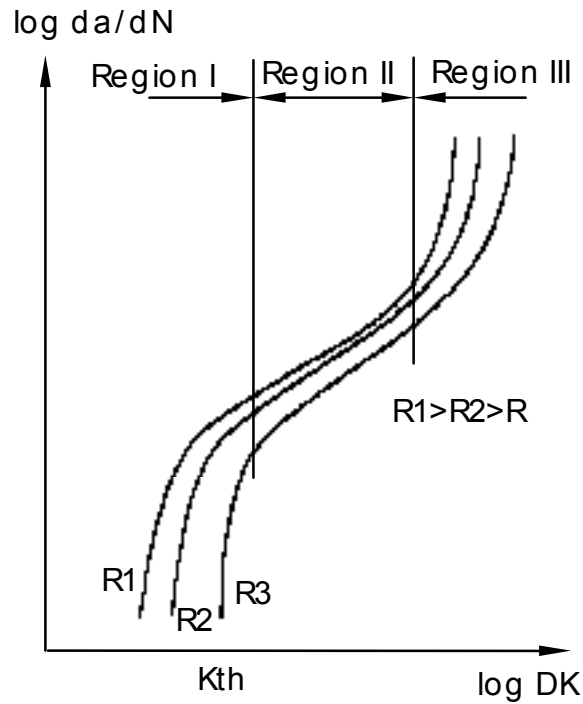


Fig.1 Schematic of fatigue crack growth rate against stress intensity factor range for constant amplitude loading for different stress ratio.

Although the plasticity induced crack closure mechanism is very effective in accounting for the fatigue crack growth behaviour in Region II<sup>3 4</sup>, it is not very successful in accounting for the threshold behaviour based only on the plastic deformation at the crack tip since the plastic deformation is now close to the scale of metallurgical irregularities. The roughness and environment induced crack closure mechanism play the same or even more important roles than the plasticity induced crack closure mechanism in the near the threshold region. The roughness and environment induced crack closure are determined by the material property and environment. Different material differs significantly. In addition, the maximum stress intensity factor may also contribute to the roughness and environment induced crack closure since the crack growth mode may change at very low stress level<sup>5</sup>.

Recent investigations on the fatigue crack growth threshold showed that a material dependent “intrinsic” threshold may exist for high stress ratios. Experimental observations also showed an effect of maximum stress intensify factor on the fatigue crack growth threshold. It seems that the conventional single threshold definition, which accounts only for the effect of stress range, may not be adequate in determining the crack growth thresholds. In this paper, a system of simplified mathematical solution is proposed based on a new dual threshold concept, the stress range threshold and the maximum stress threshold. The solution is extended for statistical aspect to deal with scatters usually accompanying the experimental threshold results

### **Features of the threshold**

It has been observed that the threshold will increase with the decrease of the stress ratio for some metals. A typical example for the experimental threshold value for 2024 T3 aluminium alloy <sup>6</sup> as function of the stress ratio is shown in Fig.2a. The threshold is reduced when the stress ratio is increased. The threshold can then be stabilised at a stress ratio larger than about  $R = 0.7$ , approaching a constant value. Further increase of the stress ratio larger than  $R = 0.9$  may lead to an excessive increase in the maximum stress intensity so that the static failure mechanism may be involved, resulting in a further reduce of threshold.

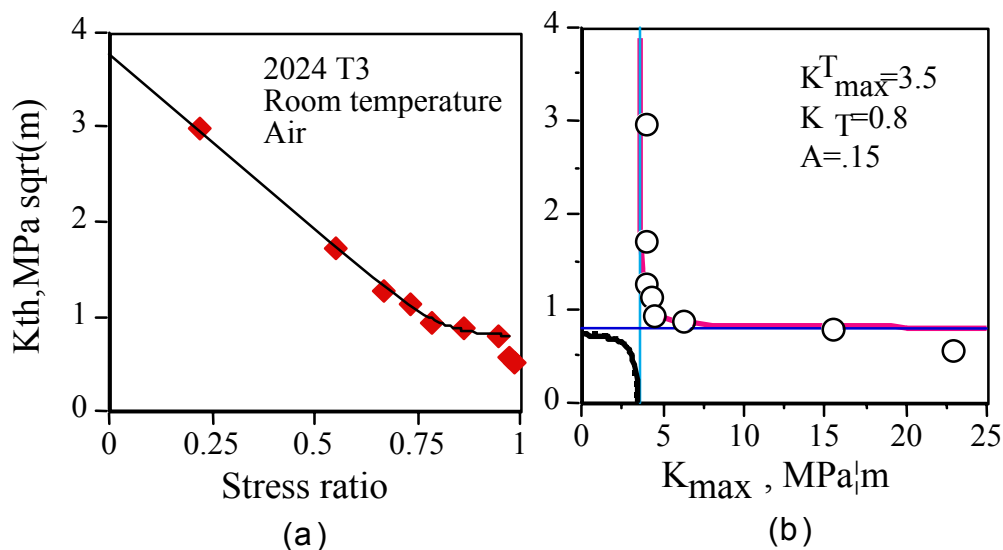


Fig.2 Comparison of experimental thresholds (symbols) with mathematical model (curves) as functions of stress ratio and maximum stress intensity factor for 2024 T3 alloy.

When the experimental results are expressed as a function of maximum stress intensity, the whole range of threshold seems to be mainly determined by two parameters with

different physical interpretations. One parameter is a stabilised threshold corresponding to the high stress ratio region within which the threshold keeps approximately constant. Another parameter appears to be a barrier of the maximum stress intensity. The threshold value will change significantly when the maximum stress intensity approaches to this barrier.

Different experimental methods may affect the experimental threshold results. An investigation in ref. <sup>7</sup> compared the results from three experimental methods to determine thresholds. Three methods; The ASTM load shedding method<sup>8</sup>, the crack prepared in compressive fatigue loading<sup>9</sup>, as well as the decrease of  $\Delta K$  at constant  $K_{\max}$ <sup>10</sup>, have been investigated. The results are shown in Fig.3. This investigation showed that the experimental methods have basically no effect on the fatigue crack growth thresholds for high stress ratios, especially the region where the threshold may be stabilised. Discrepancy appears to be at the low stress ratio region where the ASTM loading shedding method may result in high threshold, perhaps due to the excessive crack closure induced by the method.

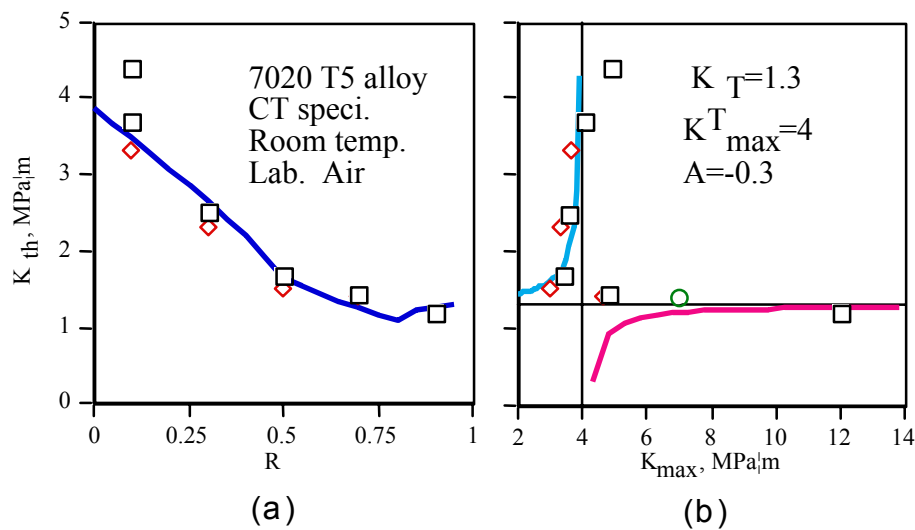


Fig.3 Comparison of experimental thresholds (symbols) with mathematical model (curves) as functions of stress ratio and maximum stress intensity factor for 7020 T5 alloy.

When the experiment results for 7020 T5 alloy is expressed as the function of maximum stress intensity factor in Fig.3b, they seem to be quite different from those of 2024 T3 alloy. In the range of small  $K_{\max}$ , the threshold seems to increase with the increase of  $K_{\max}$  before a barrier is crossed. When  $K_{\max}$  is larger than a certain level, the threshold  $\Delta K_{th}$  seems to be stabilised. For this case, two parameters can still be observed for the whole range of  $\Delta K_{th}$ . The same as for 2024 T3 alloy, a barrier of  $K_{\max}$  and a stabilised

$\Delta K_{th}$  are observed. To name the barrier of  $K_{max}$  after  $K_{max}^T$  and the stabilised  $\Delta K_{th}$  after  $\Delta K_T$ , the corresponding values for 2024 T3 and 7020 T5 are shown in the insert of Fig.2b and Fig.3b. The comparison between 2024 T3 and 7020 T5 alloy for both  $K_{max}^T$  and  $\Delta K_T$  shows that 7020 T5 alloy has generally better threshold than 2024 T3 alloy since both  $K_{max}^T$  and  $\Delta K_T$  are larger for 7020 T5 than for 2024 T3.

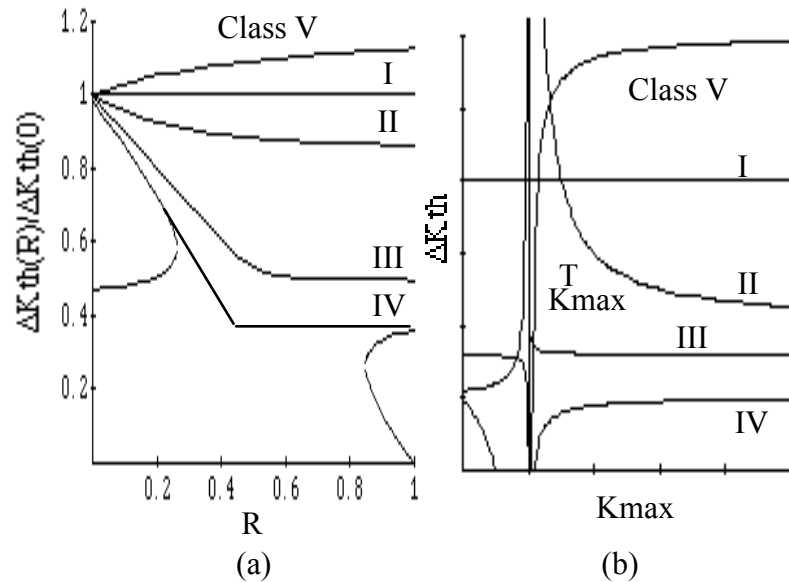


Fig.4 Schematic of threshold classification as function of stress ratio and maximum stress intensity factor.

Different relation may exist between  $\Delta K_{th}$  and  $R$ -ratio and  $K_{max}$  for different materials. According to the classification proposed in ref.<sup>11</sup>, five main classes may be identified as Fig.4a shows.  $\Delta K_{th}$  can be a constant, independent of  $R$ -ratio (Class I),  $\Delta K_{th}$  can be approximately constant for  $R$ -ratio larger than a low value of 0.5 (Class II).  $\Delta K_{th}$  can follow a 45° slope before the stabilised value is approached (Class III).  $\Delta K_{th}$  can follow a much deeper slope than 45° slope (Class IV).  $\Delta K_{th}$  can even increase with the increase of  $R$ -ratio (Class V). Whatever the classification is for  $\Delta K_{th}$ , the two parameters can still be observed when  $\Delta K_{th}$  is expressed as a function of  $K_{max}$  as Fig.4b shows for different classes. The increasing publications show that  $\Delta K_T$  may be used as an “intrinsic” material parameter, so as for  $K_{max}^T$ , which are mainly determined by the material instead of load manner. It is therefore possible to determine the  $\Delta K_{th}$  based on parameters of  $K_{max}^T$  and  $\Delta K_T$  which can be considered to be basic material constants.

### **Mathematical formations**

It has been recognised that the threshold may be stabilised for high stress ratio. Experiments also showed that the maximum stress intensity level, the  $K_{max}$ , may have a value for which the threshold may change dramatically. It can be rationalised that a  $K_{max}$

barrier can exist so that a schematic of crack growth threshold can be shown in Fig.5 as well as Fig.2-4 in the relationship between the threshold  $\Delta K_{th}$  and the maximum stress intensity  $K_{max}$ .

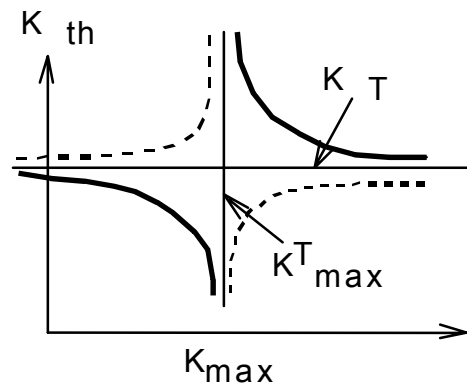


Fig.5 Schematic of the threshold model based on double threshold concept.

The threshold may follow the solid curves as for the example of 2024 T3 alloy shown in Fig.2, or the dashed curves as for example of 7020 T5 alloy shown in Fig.3, depending on the material type. When the material follows the solid curves, the threshold may gradually reduce with the increase of maximum stress intensity factor in the beginning. This behaviour may be difficult to be experimentally demonstrated since the growth of crack will increase the maximum stress intensity so that the barrier, the  $K_{max}^T$  will be rapidly approached, resulting a high threshold value to stop the crack growth. To overcome the barrier, larger load is required. When the maximum stress intensity overcomes the barrier  $K_{max}^T$ , the threshold will then decrease with the increase of the maximum stress intensity. A stabilised threshold, the  $\Delta K_T$ , may be approached (see Fig.5).

When the material follows the dashed curves, the threshold will increase with the increase of the maximum stress intensity until the barrier  $K_{max}^T$  is approached. After the barrier, the threshold will rebuild up from a low level to approach the stabilised threshold  $\Delta K_T$ . In either case, a barrier is existed at  $K_{max}^T$  to arrest the crack growth if the initial maximum stress intensity is less than  $K_{max}^T$ . This formulation has an interesting feature that a crack may be initiated at low load level but stopped when  $K_{max}$  is approaching  $K_{max}^T$ .

The fatigue crack growth threshold can be generally expressed as a function of  $K_{max}$ ,  $R$ -ratio, and  $\Delta K_T$

$$\Delta K_{th} = f(K_{max}, \Delta K_T, R) \quad (1)$$

Here,  $K_{\max}$  and  $\Delta K_T$  are considered to be intrinsic material parameters. According to the schematic of Fig.5, a three-parameter threshold model can be assumed

$$\Delta K_{th} = \begin{cases} A / (K_{\max} - K_{\max}^T) + \Delta K_T, & \text{if } \Delta K_{th} > 0 \\ 0 & \text{otherwise} \end{cases} \quad (2)$$

In this model,  $K_{\max}^T$  is a material parameter, represent a rapid rise of  $\Delta K_{th}$  when  $K_{\max}$  approaches  $K_{\max}^T$ . This parameter characterises the effect of  $K_{\max}$  to the threshold  $\Delta K_{th}$ . When  $K_{\max}^T$  approaches negative infinite,  $K_{\max}$  will then have no effect to  $\Delta K_{th}$ . This case represent Class I in Fig.4.  $\Delta K_T$  is an approaching line of  $\Delta K_{th}$  when the effect of it is diminished. For some materials, this value is measurable. A parameter of  $A$  is used in eq.(1) to account for the interaction between  $K_{\max}^T$  and  $\Delta K_T$ .

This model can account for different classifications of fatigue crack growth threshold behaviour as shown in Fig.4. In this model, the crack growth threshold is determined using two parameters, a cyclic crack growth threshold  $\Delta K_T$ , and a static crack growth threshold  $K_{\max}^T$ . Here, both the cyclic crack growth threshold and the static crack growth threshold are independent of the load ratio. The load ratio effect is accounted for with  $K_{\max}$  since  $K_{\max}$  is related to the stress ratio  $R$ . The parameter  $A$  is determined by the material systems and environment.

$\Delta K_{th}$  can also expressed as a function of stress ratio by taking account for  $\Delta K_{th} = K_{\max}(1 - R)$  at the threshold condition. Solving eq.(2) by substitution of  $\Delta K_{th}$  for  $K_{\max}$  gives

$$\Delta K_{th} = \frac{1}{2} \left\{ K_{\max}^T (1 - R) + \Delta K_T + \sqrt{D} \right\} \quad (3)$$

where

$$D = \left[ K_{\max}^T (1 - R) + \Delta K_T \right]^2 - 4(1 - R)(K_{\max}^T \Delta K_T - A) \quad (4)$$

There is no real solution for  $D < 0$  in this solution as Case IV in Fig.4 shows. To keep a continuous conservative solution, the real part may be used for  $D < 0$  as

$$\Delta K_{th} = \frac{1}{2} \left\{ K_{\max}^T (1 - R) + \Delta K_T + \text{Re}[D] \right\} \quad (5)$$

to approximate  $\Delta K_{th}$  for all the stress ratio range. The solid curve in Fig.3 is an example of this approximation. The result seems to be acceptable.

For a special case when the stress ratio is equal to zero, the crack growth threshold can be solved as

$$\Delta K_{th}(R=0) = K_{max} = \frac{1}{2} \left\{ K_{max}^T + \Delta K_T \pm \sqrt{(K_{max}^T - \Delta K_T)^2 + 4A} \right\}. \quad (6)$$

This value is determined only by material parameters  $K_{max}^T$ ,  $A$  and  $\Delta K_T$ .

To verify the present mathematical model, various materials will be analysed in the following section for the threshold behaviour.

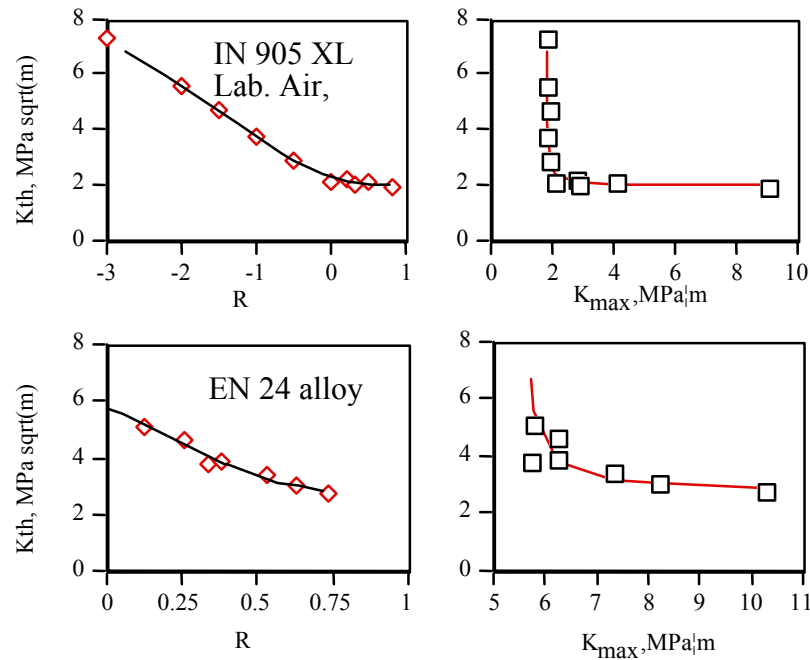


Fig.6 Comparison of experimental thresholds (symbols) with the threshold model (curves) for IN 905 alloy and EN 24 alloy.

### Applications

The advantage of the proposed model is that the basic parameters in this model have clearly defined physical interpretation. In this model,  $\Delta K_T$  corresponds an intrinsic crack growth threshold when the effect of maximum stress intensity factor is reduced.  $\Delta K_T$  is usually the stabilised stress intensity factor for high stress ratio for many materials. This value can be used as a material constant to feature the resistance of material microstructure to the growth of fatigue crack. Here,  $K_{max}^T$  is conceived as another crack growth threshold, featuring the arrest of fatigue crack growth when the applied maximum stress intensity is below this value. The effect of  $K_{max}^T$  can also be explained as a threshold when the crack growth mode may be changed due to too small tensile plastic deformation at the crack tip that leads to increased roughness and oxidation around the crack tip. The  $K_{max}^T$  can also be used as a material constant since different material has different  $K_{max}^T$ .  $A$  in the model is a parameter to determine the interaction between  $\Delta K_T$

and  $K_{\max}^T$ . In this section, the basic model given in previous section will be used for different material to rationalise and demonstrate that the fatigue crack growth threshold may be characterised using the intrinsic thresholds of  $\Delta K_T$  and  $K_{\max}^T$  for different materials.

Let us use some materials for which the thresholds can be stabilised at high stress ratio (usually for  $R > 0.6$ ). These materials are classified as Class II, II, or IV as shown in Fig.4. IN 905 XL Al alloy<sup>12</sup> is the first example since the available experimental threshold results cover an extensive range of  $-3 < R < .9$ . The experimental results are shown in Fig.6 for the laboratory air and room temperature. An almost linear relation is observed for the thresholds for the stress ratio less than zero while the threshold is nearly stabilised for the stress ratio larger than zero. When the threshold results are expressed as a function of the maximum stress intensity factor, thresholds of  $\Delta K_T$  and  $K_{\max}^T$  can be clearly observed, see Fig.6. The corresponding parameters are given in Table 1. For this material,  $\Delta K_T$  is about 1.95 and  $K_{\max}^T$  is about 1.8. The interaction parameter  $A$  is a small value of about 0.1, indicating a weak interaction between  $\Delta K_T$  and  $K_{\max}^T$ . The solid curves in Fig.6 are from the model. A very good agreement can be seen when the threshold is expressed as a function of either the stress ratio or the maximum stress intensity factor.

For the EN 24 alloy<sup>13</sup>, the experimental results in Fig.6 show that the threshold is a decreasing function of the stress ratio. There seems no stabilised threshold for high stress ratio. In another word,  $\Delta K_T$  cannot be observed based on the limited experimental results for this alloy. When the experimental results are plotted against the maximum stress intensity factor, it can be observed that the experimental results are approaching to a stabilised value, the  $\Delta K_T$ . A significant increase of threshold is also observed for the low maximum stress intensity range, indicating the existence of  $K_{\max}^T$  threshold. The fitted  $\Delta K_T$  is about 2.7 and  $K_{\max}^T$  is about 5.5 (Table 1). The parameter  $A$  is about 0.8, indicating a relatively strong interaction between  $\Delta K_T$  and  $K_{\max}^T$ . The model is good compared to the experimental results as the solid curves in Fig.6 show.

For materials of S55C and SM41B<sup>14</sup>, the experimental results show that a low threshold may exist when the maximum stress intensity factor is below the threshold of  $K_{\max}^T$  as Fig.7 shows when the experimental threshold is expressed as a function of the maximum stress intensity factor. Especially, the thresholds are observed to become small with the decrease of the maximum stress intensity factor for SM41B. This behaviour can be modelled as the schematic in Fig.5 shows. The rapid decrease in the threshold from the model is difficult to be verified since the corresponding crack growth will soon increase the maximum stress intensity factor until  $K_{\max}^T$  is approached. The intrinsic thresholds of

$\Delta K_T$  and  $K_{\max}^T$  can still be observed as the experimental results in Fig.7 show except that the threshold becomes now smaller for the stress intensity factor approaching and leaving  $K_{\max}^T$ . The threshold becomes very large when the maximum stress intensity factor crosses  $K_{\max}^T$ . We can clearly see here that  $K_{\max}^T$  is actually a barrier, perhaps characterising some microscopic feature of the material.

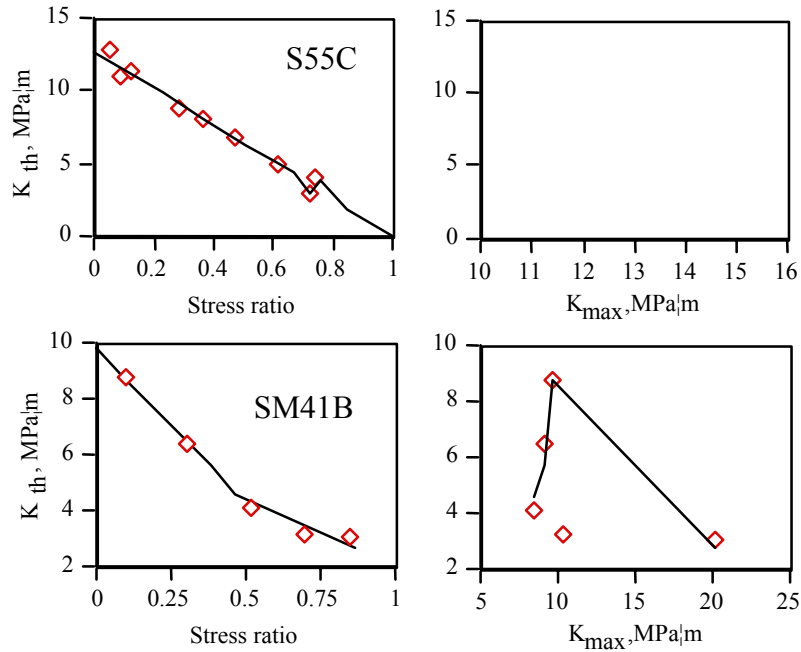


Fig.7 Comparison of experimental thresholds (symbols) with the threshold model (curves) for S55C alloy and SM41B alloy.

For the material of S55C (ref.13), the fitted  $\Delta K_T$  is about 3.5 and  $K_{\max}^T$  is about 12.5 (Table 1). The parameter  $A$  is about 1, indicating a relatively strong interaction between  $\Delta K_T$  and  $K_{\max}^T$ . This model is good compared to the experimental results as the solid curves in Fig.7 show. This material seems to have a good threshold feature at a maximum stress intensity factor of about  $12.5 \text{ MPa}\sqrt{m}$ . However, when the material is subjected to a spectrum loading with large number of cycles away from the maximum stress intensity factor of  $12.5 \text{ MPa}\sqrt{m}$ , the threshold will be significantly small. The present model can be used to reasonably represent such a feature in the threshold region as the solid curves in Fig.7 show.

For the material of SM41B, the experimental results show that a linear relation between the threshold and the stress ratio may exist for the stress ratio less than 0.5, see symbols in Fig.7. The stabilised threshold, the  $\Delta K_T$  can be experimentally observed when the threshold is expressed as a function of both the stress ratio and the maximum stress intensity factor. This material differs from other materials in that the threshold increases

with the increase of the maximum stress intensity factor when it is less than  $K_{\max}^T$ . This feature is characterised by a negative value of the interaction parameter  $A$ . The threshold is rapidly stabilised at  $\Delta K_T$  when the maximum stress intensity factor is larger than  $K_{\max}^T$ . The fitted  $\Delta K_T$  is about 3 and  $K_{\max}^T$  is about 10.1 (Table 1). The parameter  $A$  is about -2.5, indicating a strong negative interaction between  $\Delta K_T$  and  $K_{\max}^T$ . Solid curves in Fig.7 represents the results from the model that compare reasonably well to the experimental results.

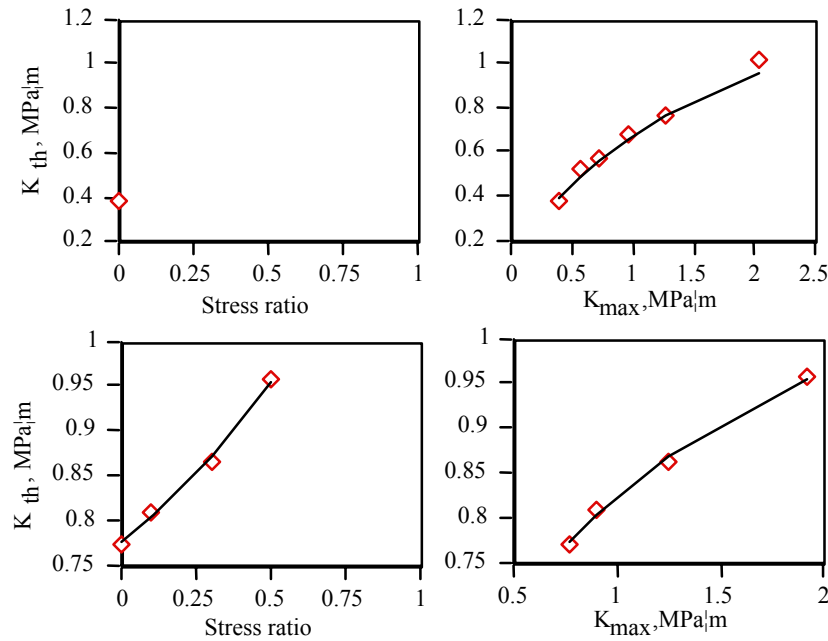


Fig.8 Comparison of experimental thresholds (symbols) with the threshold model (curves) for polycarbonate and rubber-modified polystyrene.

The model can even be extended to non-metallic materials for which significantly different threshold behaviour may be observed. Fig.8 shows two examples. The symbols in the figure represent experimental data for a polycarbonate material<sup>15</sup> and a rubber-modified polystyrene material<sup>16</sup>. The experimental results show that thresholds for these materials will increase with the increase of the stress ratio. When the test results are plotted against the maximum stress intensity factor, the threshold appears to increase with the increase of the maximum stress intensity factor. No stabilised  $\Delta K_T$  and  $K_{\max}^T$  can be experimentally determined. According to the proposed threshold model, it is found that  $\Delta K_T$  is about 1.92.  $K_{\max}^T$  is about -2.5 for polycarbonate material, see Table 1. The interaction parameter for the material is about  $A = -4.5$ . There is a very strong interaction between  $\Delta K_T$  and  $K_{\max}^T$ . For this material, low maximum stress intensity factors correspond low thresholds. The threshold model is good for such a material as the solid curves in Fig.8 show. For the rubber-modified polystyrene material, it is found that

$\Delta K_T$  is about 1.27 and  $K_{\max}^T$  is about -2, and  $A$  is about -1. This material has less interaction between  $\Delta K_T$  and  $K_{\max}^T$ . The threshold is slightly better. The results from the model are shown in Fig.8 as solid curves that fit well to the experimental results.

Table 1, Threshold parameters for different materials in  $MPa\sqrt{m}$

Material	$\Delta K_T$	$K_{\max}^T$	A
IN 905 XL Alloy	1.95	1.8	0.1
EN 24, $\sigma_y = 1275$ MPa	2.7	5.5	0.8
S55C, $\sigma_y = 399$ MPa	3.5	12.5	1
SM41B, $\sigma_y = 281$ MPa	3	10.1	-2.5
Rubber-Modified Polystyrene	1.27	-1.25	-1
Polycarbonate	1.95	-2.5	-4.5

### **Statistical feature**

There is a large scatter in the experimental results of  $\Delta K_{th}$  for different materials<sup>17</sup>. The scatter depends strongly on the stress ratio. The lower the stress ratio is, the larger the scatter may be observed. According to the crack closure concept, the low stress ratio will cause more crack face contacts to prevent the crack tip reverse yielding. For a very low  $\Delta K$ , not only the previously plastically deformed stretches, which is influenced by previous loading procedure, but also the irregularities due to microstructure inhomogeneity and environment on the crack surface will increase the crack surface contacts at low stress ratios. The effect of these random quantities on the fatigue crack growth will be magnified at reduced stress ratios. The irregular crack closure will lead to a large scatter in experimental threshold results at low stress ratios.

The significance of  $\Delta K_{th}$  is that it provides a threshold below which the fatigue crack will possibly stop growing. However, a large scatter at the low stress ratio makes this definition less meaningful. For example,  $\Delta K_{th}$  may be between 6~12Mpa $\sqrt{m}$  for a zero stress ratio loading for Fe and Ni alloys. A crack may or may not permanently stop growing at the deterministic crack growth threshold.

A correct material parameter should reveal the physical mechanism behind a phenomenon, not just a quantity with a large scatter.  $\Delta K_{th}$  is not suitable to be used as a value to determine the crack growth arrest condition since the effect of random irregularities on  $\Delta K_{th}$  may be at the same magnitude of the effect of mechanical mechanism that leads to the fatigue crack growth. Besides,  $\Delta K_{th}$  is also of stress ratio dependent. It is difficult to determine the scatter in the threshold as a function of the stress ratio.

The crack closure can be reduced with increasing the stress ratio for many materials. The scatter in the experimental  $\Delta K_{th}$  can also be effectively reduced with the increase at the stress ratio when  $\Delta K_{th}$  is approaching to  $\Delta K_T$ . Since the parameter  $\Delta K_T$  represents the cyclic feature of the threshold, it is reasonable to account for the scatter in  $\Delta K_T$  as a material property. It is also reasonable to account the scatter in  $K_{max}^T$  as another material property since  $K_{max}^T$  appears to be a material constant.

These two thresholds,  $\Delta K_T$  and  $K_{max}^T$ , can be called "intrinsic" which mainly represent the resistance of microstructure to the fatigue crack growth. The  $\Delta K_T$  can be assumed to be independent of the influence of crack closure. It may represent a cyclic crack growth threshold for a crack growing at the high stress ratio while  $K_{max}^T$  seems to be a static turning point to determine whether a substantial crack growth change may occur for the stress level approaching  $K_{max}^T$ . A randomised expression can be assumed according to the threshold model of eq.(2) as

$$\Delta K_{th} = \begin{cases} A / (K_{max} - Z_s K_{max}^T) + Z_c \Delta K_T, & \text{if } \Delta K_{th} > 0 \\ 0 & \text{otherwise} \end{cases} \quad (7)$$

In this expression,  $Z_c$  is a random variable to characterise the cyclic threshold  $\Delta K_T$ , and  $Z_s$  a random variable to characterise the static threshold. In this relation, the interaction parameter  $A$  is assumed to be deterministic to simplify the model. The random variable  $Z$  can be assumed to have a lognormal distribution with a unit mean value and a deviation of  $\sigma$  so that its probability distribution function can be expressed as

$$P_Z[\zeta < Z] = \int_0^Z \frac{1}{\sqrt{2\pi}\sigma\zeta} \exp\left\{-\frac{\ln^2 \zeta}{2\sigma^2}\right\} d\zeta. \quad (8)$$

A substitute of  $\zeta = u^\sigma$  in the above equation yields

$$P_Z[\zeta < Z] = P_Z[u < U^\sigma] = \int_0^{U^\sigma} \frac{1}{\sqrt{2\pi}u} \exp\left\{-\frac{\ln^2 u}{2}\right\} du. \quad (9)$$

This relation shows that all the log-normal random variables are linear related by a variable  $u$  which has a common distribution density in a probability density function

$$f(u) = \frac{1}{\sqrt{2\pi}u} \exp(-\ln^2 u / 2) \quad (10)$$

After the substitution of  $Z_i = u^{\sigma_i}$  in eq.(7) where  $i$  stands for  $s$  or  $c$ , the randomised  $\Delta K_{th}$  can be expressed as

$$\Delta K_{th} = \begin{cases} A / (K_{max} - u^{\sigma_s} K_{max}^T) + u^{\sigma_c} \Delta K_T, & \text{if } \Delta K_{th} > 0 \\ 0 & \text{otherwise} \end{cases} \quad (11)$$

The distribution of  $\Delta K_{th}$  can be solved by

$$P[\Delta K \leq \Delta K_{th}] = \int_0^{U(\Delta K_{th})} f[\Delta K_{th}(u)] du \quad (12)$$

where

$$f[\Delta K_{th}] = \begin{cases} [A \sigma_s u^{\sigma_s - 1} / (K_{max} - u^{\sigma_s} K_{max}^T)^2 + \sigma_c u^{\sigma_c - 1} \Delta K_T] f(u), & \text{if } \Delta K_{th} > 0 \\ 0 & \text{otherwise} \end{cases} \quad (13)$$

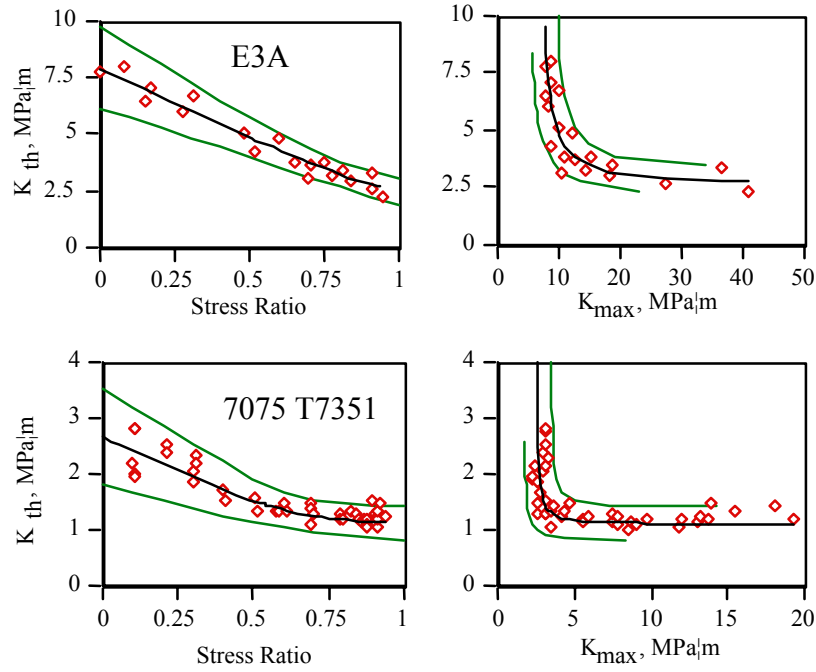


Fig.9 Comparison of experimental thresholds (symbols), the threshold model (curves), and the statistical solution of  $3\sigma$  envelope (dashed curves) for E3A and 7075 T7351.

The integration end  $U(\Delta K_{th})$  in eq.(12) is solved from the relation

$$A / (K_{max} - U^{\sigma_s} K_{max}^T) + U^{\sigma_c} \Delta K_T - \Delta K_{th} = 0 \quad \text{for } \Delta K_{th} > 0 \quad (14)$$

When the stress ratio is used instead of  $K_{max}$ ,  $f[\Delta K_{th}]$  can be solved from eq.(12) in a form of

$$f(\Delta K_{th}) = \frac{\partial \Delta K_{th}}{\partial u} f(u) \quad (15)$$

Now, we can see that the randomise  $\Delta K_{th}$  solution depends only on the scatter in the intrinsic threshold  $\Delta K_T$ , the  $\sigma_c$ , and the scatter in the load level threshold  $K_{max}^T$ , the  $\sigma_s$ . This solution not only simplifies the statistical evaluation of  $\Delta K_{th}$ , but also gives involved parameters a clear physical definition. The threshold of  $\Delta K_T$  and  $K_{max}^T$  depends on different physical mechanisms.  $\Delta K_T$  is mainly determined by the intrinsic material resistance of crack growth for a tensile cyclic loading. It is closely related to the reverse yielding ahead of the crack tip. The threshold  $K_{max}^T$  on the other hand determines a turning point at which the crack growth mode may be changed and the crack closure may increase so that the crack growth driving force is significantly reduced.

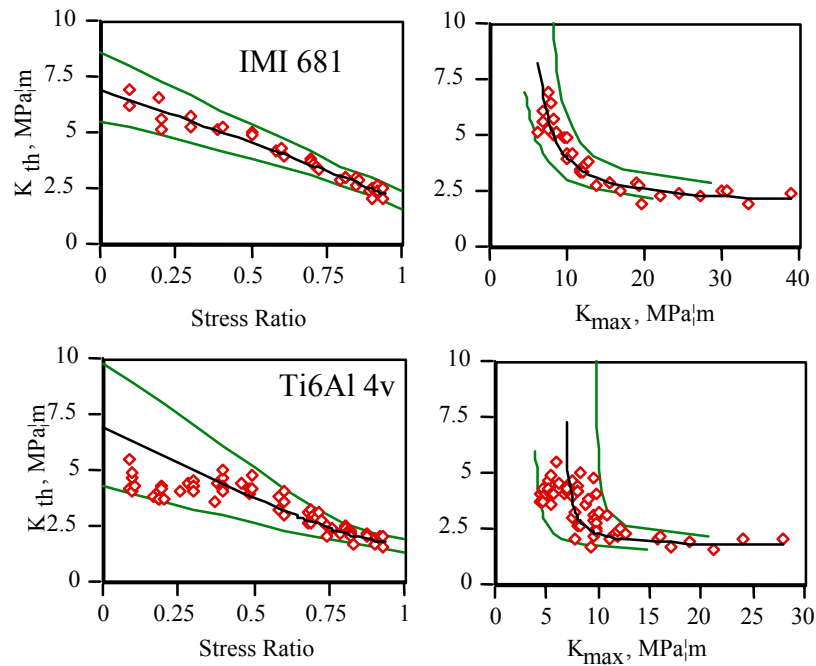


Fig.10 Comparison of experimental thresholds (symbols), the threshold model (curves), and the statistical solution of  $3\sigma$  envelope (dashed curves) for IMI 681 and Ti6Al 4V

or the experimental data of E3A<sup>18</sup>, the threshold parameters are given in Table 2. This material shows clearly the double threshold behaviour in the relation between  $\Delta K_{th}$  and  $K_{max}$  as Fig.9 shows. The estimated mean  $\Delta K_T$  is about 2.5, and the mean  $K_{max}^T$  is about 6.5. The interaction parameter  $A$  is about 7.5. This material shows a strong interaction between  $\Delta K_{th}$  and  $K_{max}$ . The standard deviation for  $\Delta K_T$  is about  $\sigma(\Delta K_T) = 0.2$  and the standard deviation for  $K_{max}^T$  is about  $\sigma(K_{max}^T) = 0.7$ . The dashed curves in Fig.9 show the  $3\sigma$  envelope for the threshold. Generally, the solution gives a good description about the scatter in the threshold region as a function of both the stress ratio and the maximum stress intensity factor. The solution also shows the same tendency that the scatter in the threshold value will increase with the decrease of the stress ratio. This tendency is due to the magnified variation effect of  $K_{max}^T$  at low stress ratios when  $K_{max}$  is approaching  $K_{max}^T$ .

(see the  $\Delta K_{th} - K_{max}$  relation shown in Fig.9). This may be the physical explanation to the increased scatter in the experimental results at low stress ratios.

Fig.9 also shows the data for 7075-T7351 alloy<sup>19</sup>. According to the experimental results,  $\Delta K_T$  is estimated to be 1.1, and  $K_{max}^T$  is about 2.5. The interaction parameter  $A$  is about 0.2. This material doesn't show much interaction between  $\Delta K_{th}$  and  $K_{max}$ . The estimate scatter for  $\Delta K_T$  is about  $\sigma(\Delta K_T) = 0.1$ , and estimated scatter for  $K_{max}^T$  is about  $\sigma(K_{max}^T) = 0.3$ , see Table 2. The dashed curves shown in Fig.9 are the  $3\sigma$  envelope from the present solution. They seem to agree with experimental results reasonably well. The same tendency is observed in the solution that the scatter in  $\Delta K_{th}$  becomes large when the stress ratio is low.

The statistical model provides different answers compared to the deterministic model about the threshold behaviour of different materials as a further comparison in Fig.10 shows for two Ti based materials. The threshold of Ti6Al 4V (ref.<sup>20</sup>) is compared to a Ti turbine disk material of IMI 685 (ref.19). The thresholds and scatters are given in Table 2. According to the experimental results, the estimated  $\Delta K_T$  about 1.6 and  $K_{max}^T$  is about 6.5 for Ti6Al 4V. The interaction parameter  $A$  for Ti6Al 4V is about 2. The estimated  $\Delta K_T$  about 1.9 and  $K_{max}^T$  is about 4.5 for IMI 685. The interaction parameter  $A$  for IMI 685 is about 12, quite different from that of Ti6Al 4V. In the deterministic method, the solid mean curves in Fig.10 show that Ti6Al 4V has almost the same threshold over all the stress ratios larger than zero.

According to the experimental results, the scatter in  $\Delta K_T$  for Ti6Al 4V is estimated to be  $\sigma(\Delta K_T) = 0.1$ , and the scatter in  $\Delta K_T$  for IMI 685 is about  $\sigma(\Delta K_T) = 0.14$ . The scatter in  $K_{max}^T$  for Ti6Al 4V is about  $\sigma(K_{max}^T) = 1$ , and the scatter in  $K_{max}^T$  for IMI 685 is about  $\sigma(K_{max}^T) = 0.7$ . The scatter in  $\Delta K_T$  for Ti6Al 4V is slightly smaller than that of IMI 685 while the scatter in  $K_{max}^T$  for Ti6Al 4V is significantly larger than that of IMI 685. Based on these parameters, the  $3\sigma$  envelope estimated according to the statistical model is shown in Fig.10 as dashed curves for both materials. They agree reasonably well with experimental results. The statistical solution shows that the low  $3\sigma$  envelope of Ti6Al 4V is significantly less than that of IMI 685, indicating a poorer threshold for Ti6Al 4V than for IMI 685. The conclusion may depend on the size of sample as can be seen here that the experimental Ti6Al 4V results have a large population. The information can at least remind the user of certain caution in using the experimental data in a deterministic way since the answer may be different from a statistical consideration as the example shows. When the reliability requirement is strict, especially for the application of turbine components, the low bound of the envelope from the statistical model should be used so

that the deterministically same material may differ significantly due to their difference in scatters in the material data.

Table 2 Threshold parameters and scatters for different materials in  $MPa\sqrt{m}$

Material	$\Delta K_T$	$K_{max}^T$	$A$	$\sigma(\Delta K_T)$	$\sigma(K_{max}^T)$
Ti6Al 4V STA	1.6	6.5	2	0.1	1.0
Ti-Turbine Disk Material (IMI 685)	1.9	4.5	12	0.14	0.7
Aluminium 7075 T7351	1.1	2.5	0.2	0.1	0.3
EN 3A $\sigma_y = 303$ MPa	2.5	6.5	7.5	0.2	0.7

### **Concluding remarks**

A new double threshold model is proposed in this investigation for the analysis of fatigue crack growth. This model is based on two elements; an intrinsic cyclic threshold which corresponds the material resistance to the fatigue crack growth due to the reverse yielding at the crack tip, and a maximum stress intensity factor threshold which contributes to the possible change of crack growth mode and the crack closure mechanism when the tensile plastic deformation ahead of crack tip is small. These two thresholds are proposed as material parameters to determine the threshold condition though they may not be directly measurable for some materials.

The benefit of using such parameters as material constants is that they have their physical interpretations. The intrinsic crack growth threshold corresponds a condition at which the crack closure effect can be eliminated so that the threshold represents a closely micro structurally related property; the resistance of material to cyclic crack growth driving force. Here, the driving force for a fatigue crack growth can be rationalised by using the reverse yielding at the crack tip under the cyclic loading in a stabilised condition (no primary plastic deformation at the crack tip<sup>21</sup>). The maximum stress intensity factor threshold on the other hand represents a condition at which the crack closure may be changed due to the possible change of crack growth mode and the increasing effect of micro irregularities and environment, resulting in a reduce of crack growth driving force. Together with the intrinsic crack growth threshold, the maximum stress intensity factor threshold determines the crack arresting condition for low stress levels for which the crack tip plastic deformation is small. This parameter is also closely related to the material property.

A system of mathematical model is developed based on the double threshold concept so that only three parameters are required to determine the threshold for various different materials (not limited to metallurgical materials). The model is successfully used to

characterise the crack growth threshold for varieties of materials with significantly different features. The model is also randomised to account for the effect of scatters in both the cyclic and static thresholds on the crack growth arresting condition. The statistical model has satisfactorily accounted for and explained the observed phenomenon that the scatter in the experimentally measured thresholds may increase considerably for low stress ratios.

### **Acknowledgement**

The author is grateful for the financial support of the internal founding of FOI, the Swedish Defence Research Agency.

## References

- <sup>1</sup> W.Elber,"Fatigue crack closure under cyclic tension", Eng. Frac. Mech. Vol.2, No.1, 37-45(1970)
- <sup>2</sup> W.Elber,"The significance of fatigue crack closure",ASTM STP 486 230-242(1971)
- <sup>3</sup> G.S.Wang and A.F.Blom, "A strip model for fatigue crack growth predictions under general load conditions", *Engng. Fracture Mech.* Vol.40, No.3, pp.507-533, 1991.
- <sup>4</sup> G.S.Wang, "The plasticity aspect of fatigue crack growth", *Engng. Fracture Mech.* Vol.46, No.6, pp.909-930, 1993
- <sup>5</sup> K. Minakawa and A.J. MeEvily, "On crack closure in the near-threshold region", *Scr. Met.*, vol.15, pp.673-666,1981
- <sup>6</sup> R.A.Schmidt and P.C.Paris, Threshold for fatigue crack propagation and the effects of load ratio and frequency, *Progress in Flaw Growth and Fracture Toughness Testing*, ASTM STP 536, pp.79-94, 1973
- <sup>7</sup> R.Pippan, H.P. Stüwe and K. Golos, "A comparison of different methods to determine the threshold of fatigue crack propagation", *Fatigue*, 1994, Vol. 16, November, pp.579-582.
- <sup>8</sup> ASTM Standard Test Method for Measurement of Fatigue Crack Growth Rates (E647-93), 'Annual Book of ASTM Standards', Vol.03.01, American Society for Testing and Materials, 1993, pp.679-706.
- <sup>9</sup> S. Suresh, *Eng. Fract. Mech.* 1985, 21, 453.
- <sup>10</sup> H. Doker, V. Bachmann, and G. Marci, In "Proc. Fatigue Thresholds - Fundamentals and Engineering Applications", (Eds J. Backlund et al) EMAS, Warley, 1981, pp.45-57.
- <sup>11</sup> A.K. Vasudevan and K. Sadananda, "Classification of fatigue crack growth behavior", *Metal. & Mater. Trans. A*, Vol. 26A, pp.1221-1234, 1995
- <sup>12</sup> H. Kemper, B. Weiss, and R. Stickler, *Eng. Fract. Mech.*, 1989, vol. 32, p.591
- <sup>13</sup> R.J. Cooke and C.J. Beevers: *Mater. Sci. Eng.*, 1974, vol.13, p.201.
- <sup>14</sup> K. Tanaka: ASTM STP 1020, 1989, p.151
- <sup>15</sup> S. Arad, J.C. Radon, and L.E. Culver: *J. Mech. Eng. Sci.*, 1971, vol. 13, p. 75.
- <sup>16</sup> L. Priutt: Ph.D. Thesis, Brown University, Providence, RI, 1993
- <sup>17</sup> Liaw, P.K., Leax, T.R., and Logsdon, W.A., *Acta Metall.* 31, 1581-1587(1983)
- <sup>18</sup> K. Jerram and E.K. Priddle: *J. Mech. Eng. Sci.*, 1973, vol. 15, p. 271
- <sup>19</sup> G. Marci, "Non-propagation conditions and fatigue crack propagation threshold", *Fatigue Fract. Engng. Mater.. Struct.* vol.17, pp.891-907, 1994.
- <sup>20</sup> G. Marci, "A fatigue crack growth threshold", *Engng. Frac. Mech.* vol.41, n3, 1992, pp.367-385.

- 
- <sup>21</sup> A.U. de Koning and D.J. Dougherty, "Prediction of low and high crack growth rates under constant and variable amplitude loading", *Fatigue crack growth under variable amplitude loading* (J. Petit et al., eds.), 1989, pp.208-217.

<b>Issuing organization</b> FOI – Swedish Defence Research Agency  Structures Institute Aeronautical Division SE-172 90 Stockholm	<b>Report number, ISRN</b> FOI-R-- 0787--SE	<b>Report type</b> Scientific Report
	<b>Research area code</b> Vehicles	
	<b>Month year</b> January, 2003	<b>Project no.</b> A824671
	<b>Customers code</b> Aeronautical Research	
	<b>Sub area code</b> Aeronautical Technology	
<b>Author/s (editor/s)</b> Gengsheng Wang	<b>Project manager</b> Gengsheng Wang	
	<b>Approved by</b> Anders F. Blom	
	<b>Sponsoring agency</b> FOI	
	<b>Scientifically and technically responsible</b>	
<b>Report title</b> <b>Cyclic and Static Fatigue Crack Growth Thresholds</b>		
<b>Abstract (not more than 200 words)</b> <p>The mathematical foundation for the new double threshold concept is investigated for the analysis of fatigue crack growth. The model consists of two major elements; an intrinsic crack growth threshold which corresponds the material resistance to the fatigue crack growth due to the reverse yielding at the crack tip, and a maximum stress intensity factor threshold which contributes to the possible change of crack growth mode and the crack closure mechanism when the tensile plastic deformation ahead of crack tip is very small. These two thresholds are proposed as material parameters to determine fatigue threshold condition. The mathematical model is developed based on the double threshold concept so that only three parameters are required to determine the threshold for various different materials. The model is successfully used to characterise the crack growth threshold for varieties of materials with significantly different features. The model is also randomised to account for the scatter in fatigue crack growth thresholds. The statistical model has successfully accounted for and explained the widely observed phenomenon that the scatter in the experimentally measured thresholds may increase considerably for low stress ratios.</p>		
<b>Keywords</b> Fatigue Crack Growth, Thresholds, R ratios, Statistics, Stress Effect		
<b>Further bibliographic information</b> FMV 5 copies, SAAB Linköping 5 copies, FOI Bromma 5 copies, KTH 5 copies, LTH 5 copies, Volvo Aero 5 copies	<b>Language</b> English	
<b>ISSN</b> 1650-1942	<b>Pages</b> 20 p.	
<b>Price acc. to pricelist</b>		

<b>Utgivare</b> Totalförsvarets Forskningsinstitut - FOI  Structures Institute Aeronautical Division SE-172 90 Stockholm	<b>Rapportnummer, ISRN</b> FOI-R-- 0787--SE	<b>Klassificering</b> Vetenskaplig Rapport
	<b>Forskningsområde</b> Farkoster	
	<b>Månad, år</b> Januari, 2003	<b>Projektnummer</b> A824671
	<b>Verksamhetsgren</b> Flygteknisk forskning	
	<b>Delområde</b> Flygfarkostteknik	
<b>Författare/redaktör</b> Gengsheng Wang	<b>Projektledare</b> Gengsheng Wang	
	<b>Godkänd av</b> Anders F. Blom	
	<b>Uppdragsgivare/kundbeteckning</b> FOI	
	<b>Tekniskt och/eller vetenskapligt ansvarig</b>	
<b>Rapportens titel (i översättning)</b> Cyklisk och statisk utmattningströskel		
<b>Sammanfattning (högst 200 ord)</b>  Matematisk analys har utfört för ett nytt dubbel utmattningströskel koncept som visar två viktiga parameter som mest påverkar utmattningströskelvärde av varierande material. Ena värde beror på materials egenskap att stå emot utmattningssprick tillväxt. Den andra beror på maximal spänning nära sprickspets. Matematisk modell har utvecklades, som visar sig mycket bred användbar området.		
<b>Nyckelord</b> Utmattning, spricktillväxt, tröskelvärde, R värde, statistisks, matematisk modell, material		
<b>Övriga bibliografiska uppgifter</b>  FMV 5 kopior, SAAB Linköping 5 kopior, FOI Bromma 5 kopior, KTH 5 kopior, LTH 5 kopior, Volvo Aero 5 kopior	<b>Språk</b> Engelska	
<b>ISSN</b> 1650-1942	<b>Antal sidor:</b> 20 s.	
<b>Distribution enligt missiv</b>	<b>Pris:</b> Enligt prislista	